Proceedings of the ASME 2016 Dynamic Systems and Control Conference
DSCC2016
October 12-14, 2016, Minneapolis, Minnesota, USA

DSCC2016-9812

ROBUST POSITION CONTROL OF A QUADROTOR USING ONBOARD OPTICAL FLOW SENSOR

Qi Lu, Beibei Ren, Siva Parameswaran
Dept. of Mechanical Engineering
Texas Tech University
Lubbock, TX 79409
Email: qi.lu@ttu.edu,
beibei.ren@ttu.edu,
siva.parameswaran@ttu.edu

Qing-Chang Zhong
Dept. of Electrical and
Computer Engineering
Illinois Institute of Technology
Chicago, IL 60616
Email: zhongqc@ieee.org

ABSTRACT

In this paper, the uncertainty and disturbance estimator (UDE)-based position controllers are developed to achieve the robust position control of a quadrotor using only onboard sensing. Firstly, in order to accurately estimate the positions of the quadrotor in GPS-denied environments, an open source high speed optical flow sensor PX4FLOW is adopted. Secondly, the UDE-based controllers are developed to handle the challenges brought by the highly nonlinear quadrotor position dynamics, including underactuation, coupling, nonaffine inputs, model uncertainties and external disturbances. Real flight experiments, including hover and disturbance rejection are carried out to demonstrate the effectiveness of the developed UDE-based controllers.

INTRODUCTION

In recent years, unmanned aerial vehicles (UAVs) have drawn considerable amount of attention from both research and industrial communities because of their wide field of applications, such as search and rescue, industrial inspection, precision agriculture, aerial photography, etc [1, 2]. In order to accomplish the aforementioned tasks, the ability of the UAVs to navigate autonomously, maneuver sharply and hover precisely is very important.

One of the popular UAVs that has been widely applied is the quadrotor since it has relatively simple mechanical structure and vertically taking off (landing) ability. The quadrotor has six degrees of freedom including three rotational (attitude) and three translational (position) motions with solely four independent control inputs (thrust and three torques along the body axes). The horizontal positions of the quadrotor are controlled by varying its attitude angles. The quadrotor is able to stabilize and control its attitude angles with the information from onboard inertia measurement unit (IMU), which consists of accelerometers, gyroscopes and magnetometers. Nevertheless, even with the attitude angles stabilized to zero degrees, due to the inaccurate measurements of the low-cost onboard IMU and other environmental disturbances, the quadrotor could not hover at a fixed point for a long time. Hence, the position control of a quadrotor is an essential step towards the quadrotor autonomy.

The precise position control of a quadrotor requires the accurate estimation of the quadrotor positions followed by proper control actions [3, 4]. In order to have an accurate position estimation of the quadrotor, various position estimation sensors and methods have been investigated. The global positioning system (GPS) receiver is a common onboard device utilized for the navigation task of quadrotor UAVs [2, 5, 6]. However, the GPS receiver mainly has two constraints: 1) accuracy, and 2) a clear view of the sky. According to the National Coordination Office for Space-Based Positioning, Navigation, and Timing [7], the horizontal accuracy of the GPS receiver is about 3.5 meters. Furthermore, the requirement for a clear view of the sky has limited the GPS receiver mostly for outdoor applications. As for the GPS-denied navigation, one of the widely adopted methods for

quadrotor navigation is the motion capture system, which utilizes multiple external cameras and reflective markers to determine the positions of the quadrotor [8, 9]. However, it is not suitable for missions where the installation of such a system is not feasible. Therefore, for UAVs, how to extract their position information in GPS-denied environments solely from the onboard sensing is still a very challenging and open research topic [3].

The laser range finder [10] and onboard camera [3, 4, 11] seem to be two promising onboard solutions for the quadrotor navigation task. Compared to laser, the onboard camera has the advantage of lightweight and low cost. Recent studies have revealed that flying insects utilize optical flow to accomplish their dynamic navigation while keeping energy consumption at an unbelievable low level [12]. This biomimetic principle motivates a number of researchers exploring the idea of optical flow-based navigation [4, 11]. In [4], an open source high speed optical flow sensor PX4FLOW is developed. The sensor weighs about 20 grams with the update rate about 120 Hz in low light conditions. The lightweight and fast update rate features make it especially suitable for quadrotor navigation task. Therefore, the PX4FLOW is utilized in this paper to accomplish the quadrotor position estimation task.

Besides the difficulties of vehicle position estimation, another aspect of challenges for the position control of UAVs comes from its highly nonlinear system dynamics. First of all, the quadrotor is an underactuated multiple-input multiple-output (MIMO) system, which has six outputs while only four inputs. The horizontal positions (x, y) of the quadrotor are controlled by varying its attitude angles. Furthermore, the inputs of the horizontal position dynamics are in nonaffine forms. The coupling between the position subsystems and attitude subsystems also brings challenges to the controller design. Finally, the quadrotor is very sensitive to the perturbations caused by model uncertainty and external disturbance, which could be generated from battery voltage dropping, aerodynamic effects or wind gusts.

In order to deal with those challenges and to achieve good control performance, many control strategies have been reported in the literature. Backstepping is a well-known technique used for control of nonlinear systems and it is well suited for the cascaded structure of the quadrotor dynamics to solve the underactuation problem [13, 14]. In order to compensate the model uncertainties, adaptive control methods are widely used, such as the model reference adaptive control [15], the immersion and invariance-based adaptive control [16] and adaptation laws based on Lyapunov-like energy function [17]. The robustness is crucial to the UAVs, since they are constantly perturbed by external disturbances, specially in outdoor applications [17]. Hence, the robust control of a quadrotor is still an active field, such as sliding mode control [18], H_∞ control [19] and disturbance observer based control [20].

Compared to the aforementioned robust control methods, the uncertainty and disturbance estimator (UDE)-based controller, which was proposed in [21], has a relatively simple structure and it is computationally efficient. The basic idea of the UDE method is that in the frequency domain an engineering signal (the model uncertainty and external disturbance) can be approximated by putting it through a filter with the appropriate bandwidth. The remarkable performance of the UDE strategy has been demonstrated in recent years through both theories [22, 23, 24] and practical applications [25, 26, 27, 28].

In this paper, in response to the aforementioned challenges, the UDE-based controllers are developed for the position control of a quadrotor. The major contributions of this paper include:

1. The PX4FLOW optical flow sensor is integrated to accomplish the onboard position estimation in GPS-denied environment.
2. In order to to achieve the position control of a quadrotor while dealing with the problem of underactuation, coupling, nonaffine inputs, model uncertainties and external disturbances, a robust tracking control scheme based on the UDE is developed.
3. The effectiveness of the developed control strategy is demonstrated through real flight experiment studies. Compared with previous UDE works on quadrotor attitude and height control [25, 28], this paper mainly focuses on the horizontal position controller development.

This paper evolves along the following lines. In Section 2, the mathematical model of a quadrotor is presented and the control problem is formulated. The details of the UDE-based controller design are discussed in Section 3. In Section 4, real flight experiments, including hover at fixed point and step disturbance rejection, are carried out to demonstrate the effectiveness of the proposed approach. Conclusions are made in Section 5.

PRELIMINARIES AND PROBLEM FORMULATION

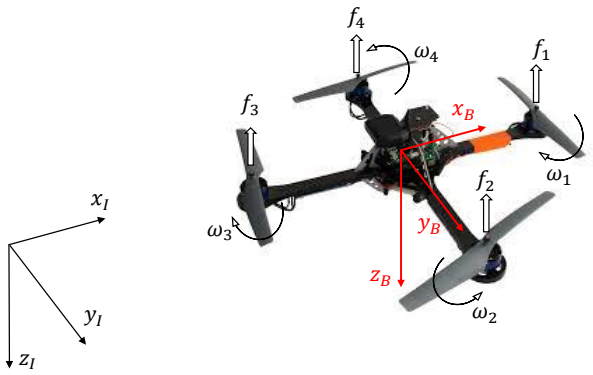

Figure 1. Coordinates system for a quadrotor

Figure 1 illustrates the composition and coordinates system of a quadrotor. The motion of the quadrotor is controlled by varying the speeds of four rotors. By varying the speeds of rotor 1 and rotor 3, the quadrotor will pitch up or down. Similarly, the roll motion could be achieved by varying the speeds of rotor 2 and rotor 4. The yaw motion of the quadrotor is achieved by varying the speeds of one pair of motors (1 and 3) and another pair of motors (2 and 4). The assumptions for the mathematical model used in this paper include: 1) the structure of the quadrotor is rigid and symmetric, and 2) the thrust and torque generated by each rotor are proportional to the square of the rotor speed. The inertia frame and body fixed frame are denoted as $\mathscr{I} = \{ x_I \; y_I \; z_I \}$ and $\mathscr{B} = \{ x_B \; y_B \; z_B \}$ respectively. The thrust f_k and torque τ_k generated by each rotor are $f_k = h_F \omega_k^2$ and $\tau_k = h_M \omega_k^2$ respectively, where ω_k is the kth motor speed, h_F and h_M are the thrust and drag constants. The total lift force F and torques τ_ϕ, τ_θ, τ_ψ along the body axes can be expressed as

$$F = f_1 + f_2 + f_3 + f_4, \quad \tau_\phi = l(f_4 - f_2)$$
$$\tau_\theta = l(f_1 - f_3), \quad \tau_\psi = \tau_2 + \tau_4 - \tau_1 - \tau_3$$

where l denotes the quadrotor arm length. The positions and attitude angles of the quadrotor in $\mathscr{I}$ are represented by x, y, z and ϕ, θ, ψ respectively. Assume that there exist bounded disturbance signals d_i, $i = 1...3$ for the position subsystems, which may be caused by some environmental factors. The position dynamics of the quadrotor could be described using the following equations [1]:

$$\ddot{x} = -\frac{F}{m}[\cos(\psi)\sin(\theta)\cos(\phi) + \sin(\psi)\sin(\phi)] + d_1 \quad (1)$$
$$\ddot{y} = -\frac{F}{m}[\sin(\psi)\sin(\theta)\cos(\phi) - \cos(\psi)\sin(\phi)] + d_2 \quad (2)$$
$$\ddot{z} = -\frac{F}{m}[\cos(\theta)\cos(\phi)] + g + d_3 \quad (3)$$

where g is the gravitational acceleration, m is the mass. The reference signals are given as $\begin{bmatrix} x_r \; y_r \; z_r \end{bmatrix}^T$, which are continuous differentiable and bounded up to their second order time derivatives. The overall control objective is to develop the UDE-based robust control algorithms for the quadrotor system to drive the states $\begin{bmatrix} x \; y \; z \end{bmatrix}^T$ to track the reference signals $\begin{bmatrix} x_r \; y_r \; z_r \end{bmatrix}^T$.

CONTROL DESIGN

UDE-based Position Controller Development

From the block diagram of the overall control system (Fig. 2), it could be seen that the cascaded inner-outer loop control structure is utilized to deal with the underactuation, where the inner loop is the attitude controller and the outer loop is the position

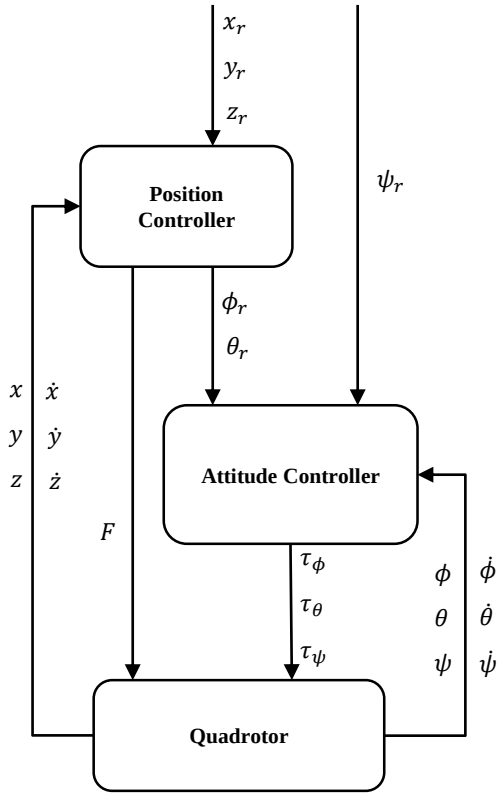

Figure 2. Quadrotor control system structure

controller. Since the design process of the attitude controllers are already discussed in the previous published paper [25], this paper will focus on the controller development for the position subsystems. From the x, y dynamics (1) and (2), it could be seen that the control inputs for horizontal motions are in nonaffine forms, which leads to the failure of using feedback linearization. Furthermore, the construction of inverse trigonometric operators may lead to singularity problems. To deal with this problem, the $\sin(\theta_r)$ and $\sin(\phi_r)$ functions are approximated by $K_x\theta_r$ and $K_y\phi_r$, respectively. The approximation errors will be handled by the UDE technique described in [22]. The virtual control inputs for the horizontal motion are designed as

$$u_x = K_x\theta_r\cos(\phi) \quad (4)$$
$$u_y = -K_y\phi_r \quad (5)$$

By choosing the generalized coordinates as $\xi_1 = x$, $\xi_2 = y$, $\xi_3 = z$, reference signals as $\xi_{r1} = x_r$, $\xi_{r2} = y_r$, $\xi_{r3} = z_r$, the position dynamics (1) (2) and (3) are rewritten as

$$\ddot{\xi}_i = -B_i u_i + \bar{g}_i + D_i \quad (6)$$

where $i = 1...3$ denote the x, y and z subsystems, $B_1 = \frac{F}{m}$, $B_2 = \frac{F}{m}$, and $B = \frac{1}{m}$ are the input constants, $\bar{g}_1 = 0$, $\bar{g}_2 = 0$, and $\bar{g}_3 = g$ denote the gravitational accelerations, $u_1 = u_x$, $u_2 = u_y$, and $u_3 = F$ are the control inputs, and

$$\begin{aligned} D_1 &= -\frac{F}{m}\left[\cos(\psi)\sin(\theta)\cos(\phi) + \sin(\psi)\sin(\phi) - u_x\right] + d_1 \\ D_2 &= -\frac{F}{m}\left[\sin(\psi)\sin(\theta)\cos(\phi) - \cos(\psi)\sin(\phi) - u_y\right] + d_2 \\ D_3 &= \frac{F}{m}\left[1 - \cos(\theta)\cos(\phi)\right] + d_3 \end{aligned} \tag{7}$$

are the lumped uncertainty terms. The position and velocity tracking errors are defined as

$$\begin{aligned} e_i &= \xi_{ri} - \xi_i \\ \dot{e}_i &= \dot{\xi}_{ri} - \dot{\xi}_i \end{aligned} \tag{8}$$

and the filtered tracking errors are defined as

$$\varepsilon_i = \Lambda_i e_i + \dot{e}_i \tag{9}$$

where Λ_i are positive design parameters. The time derivatives of Eqn. (9) are given by

$$\dot{\varepsilon}_i = \Lambda_i \dot{e}_i + \ddot{\xi}_{ri} + B_i u_i - \bar{g}_i - D_i \tag{10}$$

If all states are measurable, the controller could be designed as

$$B_i u_i = -\Lambda_i \dot{e}_i - \ddot{\xi}_{ri} + \bar{g}_i - k_i \varepsilon_i + u_i^d \tag{11}$$

using feedback linearization, with the desired error dynamics

$$\dot{\varepsilon}_i = -k_i \varepsilon_i \tag{12}$$

where k_i are positive control gains, and u_i^d are the lumped uncertainty compensation terms. If D_i are known, then the lumped uncertainty compensation terms could be designed as $u_i^d = D_i$. Nevertheless, the lumped uncertainty terms D_i in Eqn. (10) could not be directly measured due to the existence of bounded disturbance terms. Thus, u_i^d should be redesigned. Substituting (11) into (10) leads to

$$\dot{\varepsilon}_i = -k_i \varepsilon_i + u_i^d - D_i$$

Solving for the lumped uncertainty terms results in

$$D_i = -\dot{\varepsilon}_i - k_i \varepsilon_i + u_i^d$$

Following the techniques provided in [22], adopting strictly proper low-pass filters $G_i^f(s)$ with an unity gain and zero phase shift over the spectrum of D_i, the lumped uncertainty terms D_i could be approximated as

$$\hat{D}_i = \mathscr{L}^{-1}\left\{G_i^f(s)\right\} * \left[-\dot{\varepsilon}_i - k_i \varepsilon_i + u_i^d\right] \tag{13}$$

where $\mathscr{L}^{-1}\{\cdot\}$ is the inverse-Laplace transform operator and "$*$" is the convolution operator. Substituting $u_i^d = \hat{D}_i$ into (13) leads to

$$u_i^d = \mathscr{L}^{-1}\left\{G_i^f(s)\right\} * \left[-\dot{\varepsilon}_i - k_i \varepsilon_i + u_i^d\right]$$

Solving for u_i^d results in

$$u_i^d = -\mathscr{L}^{-1}\left\{\frac{G_i^f(s)}{1 - G_i^f(s)}\right\} * \left[\dot{\varepsilon}_i + k_i \varepsilon_i\right] \tag{14}$$

Combining Eqn. (11) and Eqn. (14) leads to the UDE-based position controllers

$$\begin{aligned} u_i = \frac{1}{B_i}\bar{g}_i - \frac{1}{B_i}\Bigg[&k_i \varepsilon_i + \Lambda_i \dot{e}_i + \ddot{\xi}_{ri} \\ &+ \mathscr{L}^{-1}\left\{\frac{G_i^f(s)}{1 - G_i^f(s)}\right\} * \left(\dot{\varepsilon}_i + k_i \varepsilon_i\right)\Bigg] \end{aligned} \tag{15}$$

where $i = 1...3$ denote the x, y and z subsystem, respectively.

Controller Implementation and Parameter Selection

According to [21], the choice of first order low-pass filters in the form of

$$G_i^f(s) = \frac{1}{T_i s + 1} \tag{16}$$

is practical, where T_i are the positive time constants that could be tuned to adjust the bandwidths of the low-pass filters. Since $\frac{1}{B_3}\bar{g}_3 = mg$, the gravity is compensated by a constant thrust command in implementation. c_3 is introduced as a positive constant coefficient that relates the thrust command to the generated thrust force. Thus, the input coefficient for altitude control is defined as $b_3 = \frac{c_3}{B_3}$. The roll and pitch reference angles for the attitude subsystems could be solved using Eqn. (4) and Eqn. (5) as

$$\theta_r = \frac{u_x}{K_x \cos(\phi)}, \quad \phi_r = -\frac{1}{K_y} u_y$$

Since $B_1 = B_2 = \frac{F}{m}$ and the ratio of $\frac{F}{mg}$ could be easily calculated, the input coefficients b_1 and b_2 are introduced as $b_1 = \frac{1}{K_x g}$ and $b_2 = \frac{1}{K_y g}$. Therefore, there are four parameters T_i, Λ_i, k_i and

Table 1. Control parameters

Dof	Λ	T	k	b
x	1	0.015	1	0.100
y	1	0.015	1	0.100
z	1	0.05	1	0.0010

b_i for each controller. The selection of controller parameters is listed in the Tab. 1.

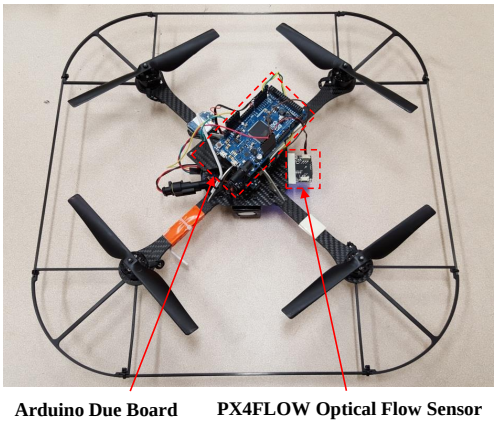

Figure 3. Experiment platform

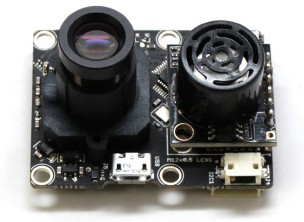

Figure 4. PX4FLOW optical flow sensor [4]

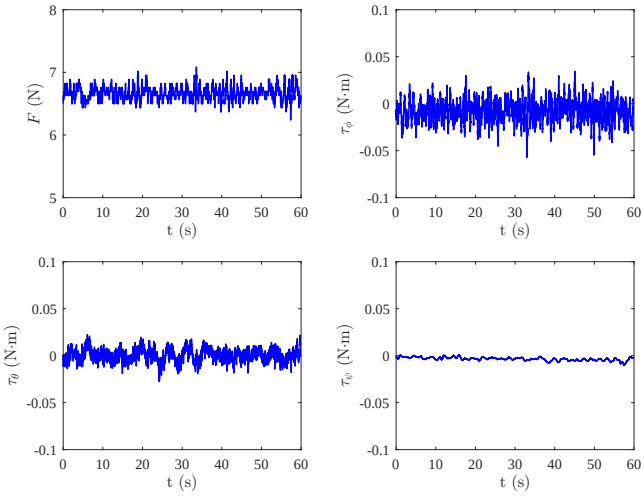

Figure 6. Control inputs for the hover at fixed point test

velocities $\dot{x}$, $\dot{y}$ and the altitude z information. The PX4FLOW is a low cost high speed open source optical flow camera [4]. It is equipped with a CMOS image sensor, a three axis gyroscope and a Maxbotix HRLV-EZ4 ultrasonic distance sensor. Since the PX4FLOW only provides the velocity measurements $\dot{x}$, $\dot{y}$, the position information x, y are estimated by integrating the velocity data. And the vertical velocity $\dot{z}$ is estimated through differentiating the ultrasonic sensor measurement z.

EXPERIMENT VALIDATION

Experiment Testbed

The Hummingbird quadrotor from Ascending Technologies GmbH (AscTec) [29] (Fig. 3) is used as the experiment platform to verify the effectiveness and performance of the developed UDE-based controllers. It has two ARM7 microprocessors onboard, i.e., low level processor and high level processor. The high level processor could access the onboard sensor data and send commands to the motors. The onboard IMU could provide the measurements for the attitude angles ϕ, θ, ψ and their velocities $\dot{\phi}$, $\dot{\theta}$, $\dot{\psi}$. For the position measurement, a PX4FlOW optical flow sensor (Fig. 4) is added, which could provide the horizontal

Table 2. RMSEs of the experiment results

Dof	Case I	Case II
x	0.048 m	0.056 m
y	0.053 m	0.056 m
z	0.024 m	0.024 m

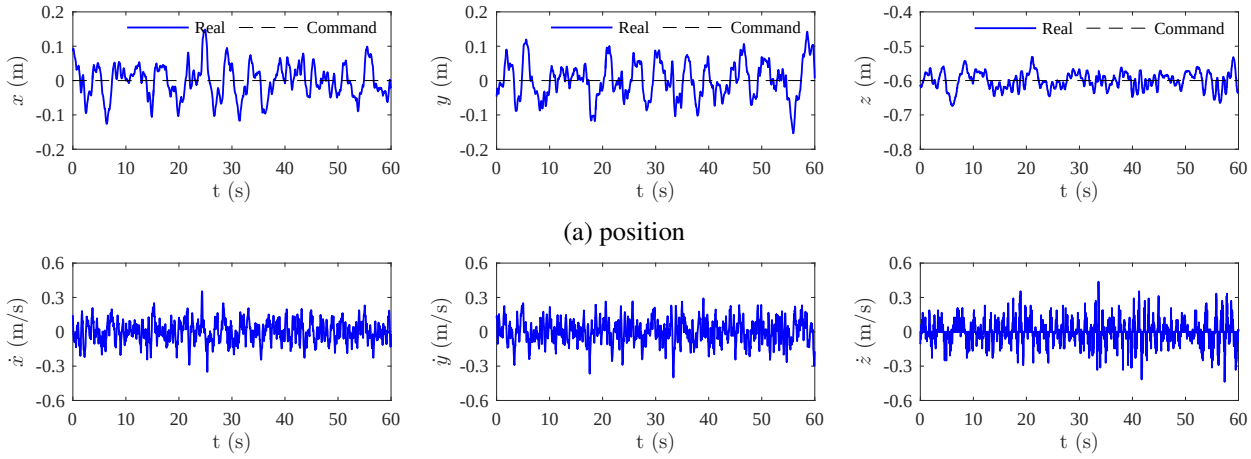

(a) position

(b) velocity

Figure 5. Hover at fixed point test

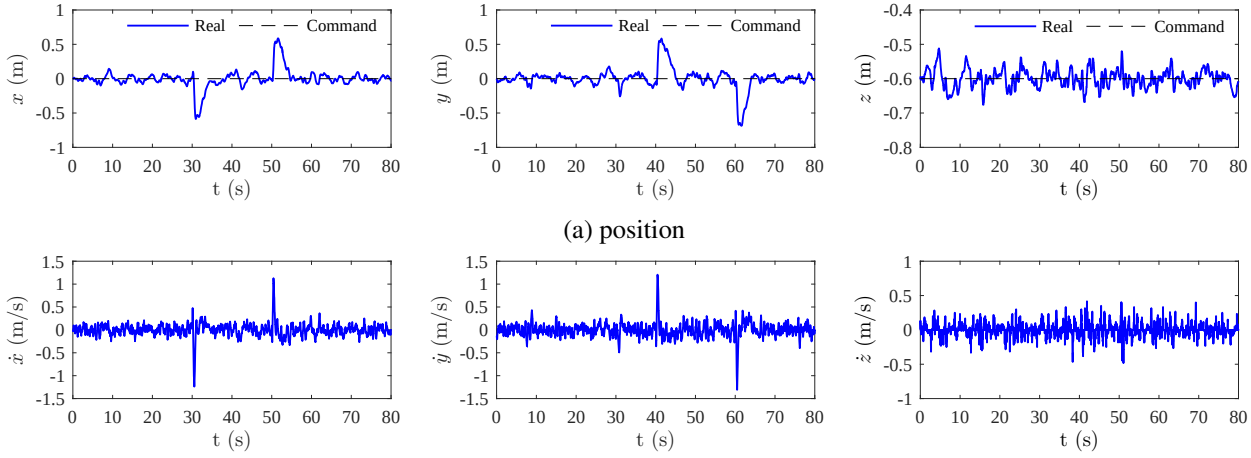

(a) position

(b) velocity

Figure 8. Step disturbance rejection

Experiment Results

Case I: Hover at Fixed Point. The objective of this experiment is to make the quadrotor hover at the desired point. The position references are set as $x_r = 0$ m, $y_r = 0$ m and $z_r = -0.6$ m, which is above the ground since the z positive axis is pointing towards the ground. Figure 5 shows the experiment results, where the first row represents the real positions and position commands. The root mean square errors (RMSEs) of the first case are presented in the second column of the Tab. 2. The velocities of the quadrotor are shown in the second row of Fig. 5. The control inputs are plotted in Fig. 6. Figure 7 shows the horizontal coordinates plot, where it could be clearly seen that the quadrotor is able to maintain its horizontal position within a circle whose radius is about 0.15 m.

Case II: Step Disturbance Rejection. The case II is carried out to demonstrate the disturbance rejection ability of the developed controller. The experiment setup and controller parameters are the same with case I. The objective of this experiment is to make the quadrotor hover at the desired point while under the effects of disturbances. The position references are set as $x_r = 0$ m, $y_r = 0$ m and $z_r = -0.6$ m. Figure 8 shows the experiment results. There are no disturbance applied in the first 30 seconds. The step input disturbance with the magnitude of 10° is applied to x controller at 30 seconds and disabled at 50 seconds and applied to y controller at 40 seconds and disabled at 60 seconds. It can be seen that the quadrotor is able to maintain stable after the disturbance is applied and recover to the desired reference point within about 7 seconds. The first row of Fig. 8

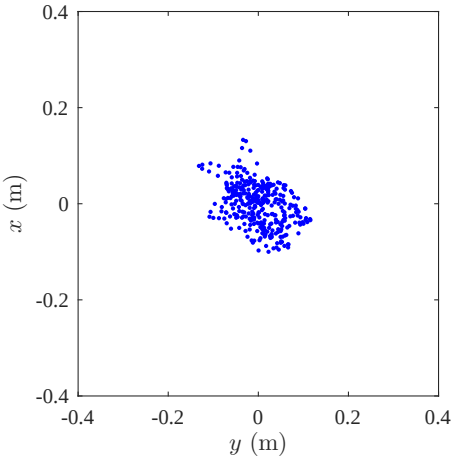

Figure 7. Horizontal coordinates plot for the hover at fixed point test

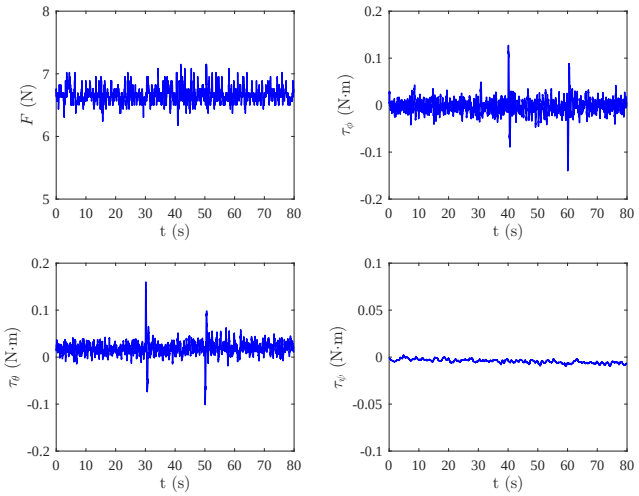

Figure 9. Control inputs for the step disturbance rejection test

shows the position variations of the quadrotor. The steady state RMSEs after the disturbance is applied are calculated in the third column of the Tab. 2. Figure 9 shows the control inputs. The experiment results have demonstrated the good robust performance of the UDE-based controllers for handling external disturbances.

CONCLUSIONS

In this paper, the UDE-based controllers were developed to achieve the robust position control of a quadrotor in GPS-denied environments. Firstly, a high-speed optical flow sensor PX4FLOW was adopted to achieve the accurate position estimation of the vehicle. Then the UDE-based controllers were developed to deal with the problems of underactuation, coupling, model uncertainty, nonaffine input and external disturbance. The effectiveness of the developed controllers has been verified through real flight experiments, including hover at fixed point and step disturbance rejection.

REFERENCES

[1] Bouabdallah, S., 2007. "Design and control of quadrotors with application to autonomous flying". PhD thesis, École Polytechnique federale de Lausanne, Lausanne, Switzerland.

[2] Hoffmann, G. M., Huang, H., Waslander, S. L., and Tomlin, C. J., 2007. "Quadrotor helicopter flight dynamics and control: theory and experiment". In Proceedings of Guidance, Navigation, and Control Conference, Vol. 2, AIAA.

[3] Mebarki, R., Lippiello, V., and Siciliano, B., 2015. "Nonlinear visual control of unmanned aerial vehicles in GPS-denied environments". *IEEE Transactions on Robotics,* ***31***(4), pp. 1004–1017.

[4] Honegger, D., Meier, L., Tanskanen, P., and Pollefeys, M., 2013. "An open source and open hardware embedded metric optical flow CMOS camera for indoor and outdoor applications". In Proceedings of International Conference on Robotics and Automation, IEEE, pp. 1736–1741.

[5] Choi, Y.-C., and Ahn, H.-S., 2015. "Nonlinear control of quadrotor for point tracking: actual implementation and experimental tests". *IEEE/ASME Transactions on Mechatronics,* ***20***(3), pp. 1179–1192.

[6] Yun, B., Peng, K., and Chen, B. M., 2007. "Enhancement of GPS signals for automatic control of a UAV helicopter system". In Proceedings of International Conference on Control and Automation, IEEE, pp. 1185–1189.

[7] National Coordination Office for Space-Based Positioning, Navigation, and Timing. GPS accuracy. `http://www.gps.gov/systems/gps/performance/accuracy/`. [Online].

[8] Michael, N., Mellinger, D., Lindsey, Q., and Kumar, V., 2010. "The GRASP multiple micro-UAV testbed". *IEEE Robotics & Automation Magazine,* ***17***(3), pp. 56–65.

[9] Goodarzi, F. A., Lee, D., and Lee, T., 2015. "Geometric adaptive tracking control of a quadrotor UAV on SE (3) for agile maneuvers". *ASME Journal of Dynamic Systems, Measurement and Control,* ***137***(9), pp. 20–32.

[10] Shen, S., Michael, N., and Kumar, V., 2011. "Autonomous multi-floor indoor navigation with a computationally constrained MAV". In Proceedings of International Conference on Robotics and Automation, IEEE, pp. 20–25.

[11] Xian, B., Liu, Y., Zhang, X., Cao, M., and Wang, F., 2014. "Hovering control of a nano quadrotor unmanned aerial vehicle using optical flow". In Proceedings of Chinese Control Conference, IEEE, pp. 8259–8264.

[12] Floreano, D., Zufferey, J.-C., Srinivasan, M. V., and Ellington, C., 2009. *Flying insects and robots*. Springer.

[13] Bouabdallah, S., and Siegwart, R., 2007. "Full control of a quadrotor". In Proceedings of the International Conference on Intelligent Robots and Systems, IEEE, pp. 153–158.

[14] Ramirez-Rodriguez, H., Parra-Vega, V., Sanchez-Orta, A., and Garcia-Salazar, O., 2014. "Robust backstepping control based on integral sliding modes for tracking of quadrotors". *Journal of Intelligent & Robotic Systems,* ***73***(1-4), pp. 51–66.

[15] Dydek, Z. T., Annaswamy, A. M., and Lavretsky, E., 2013. "Adaptive control of quadrotor UAVs: A design trade study with flight evaluations". *IEEE Transactions on Control Systems Technology,* ***21***(4), pp. 1400–1406.

[16] Zhao, B., Xian, B., Zhang, Y., and Zhang, X., 2015. "Nonlinear robust adaptive tracking control of a quadrotor UAV via immersion and invariance methodology". *IEEE Transactions on Industrial Electronics,* ***62***(5), pp. 2891–2902.

[17] Islam, S., Liu, P., and El Saddik, A., 2015. "Robust control of four-rotor unmanned aerial vehicle with disturbance uncertainty". *IEEE Transactions on Industrial Electronics,* ***62***(3), pp. 1563–1571.

[18] Lee, D., Kim, H. J., and Sastry, S., 2009. "Feedback linearization vs. adaptive sliding mode control for a quadrotor helicopter". *International Journal of Control, Automation and Systems,* ***7***(3), pp. 419–428.

[19] Raffo, G. V., Ortega, M. G., and Rubio, F. R., 2010. "An integral predictive/nonlinear H_∞ control structure for a quadrotor helicopter". *Automatica,* ***46***(1), pp. 29–39.

[20] Dong, W., Gu, G.-Y., Zhu, X., and Ding, H., 2014. "High-performance trajectory tracking control of a quadrotor with disturbance observer". *Sensors and Actuators A: Physical,* ***211***, pp. 67–77.

[21] Zhong, Q.-C., and Rees, D., 2004. "Control of uncertain LTI systems based on an uncertainty and disturbance estimator". *ASME Journal of Dynamic Systems, Measurement, and Control,* ***126***(4), pp. 905–910.

[22] Ren, B., Zhong, Q.-C., and Chen, J., 2015. "Robust control for a class of non-affine nonlinear systems based on the uncertainty and disturbance estimator". *IEEE Transaction on Industrial Electronics,* ***62***(9), pp. 5881–5888.

[23] Kuperman, A., and Zhong, Q.-C., 2010. "Robust control of uncertain nonlinear systems with state delays based on an uncertainty and disturbance estimator". *International Journal of Robust and Nonlinear Control,* ***21***(1), pp. 79–92.

[24] Stobart, R., Kuperman, A., and Zhong, Q.-C., 2011. "Uncertainty and disturbance estimator–based control for uncertain LTI-SISO systems with state delays". *ASME Journal of Dynamic Systems, Measurement, and Control,* ***133***(2), p. 024502.

[25] Dai, J., Lu, Q., Ren, B., and Zhong, Q.-C., 2015. "Robust attitude tracking control for a quadrotor based on the uncertainty and disturbance estimator". In Proceedings of Dynamic Systems and Control Conference, ASME, p. V001T06A004.

[26] Chen, J., Ren, B., and Zhong, Q.-C., 2016. "UDE-based trajectory tracking control of piezoelectric stages". *IEEE Transactions on Industrial Electronics*. DOI 10.1109/TIE.2016.2542780.

[27] Ren, B., Wang, Y., and Zhong, Q.-C., 2015. "UDE-based control of variable-speed wind turbine systems". *International Journal of Control*. DOI 10.1080/00207179.2015.1126678.

[28] Sanz, R., Garcia, P., Zhong, Q.-C., and Albertos, P., 2016. "Robust control of quadrotors based on an uncertainty and disturbance estimator". *ASME Journal of Dynamic Systems, Measurement, and Control,* ***138***(7), p. 071006.

[29] Ascending Technologies. `http://www.asctec.de/en/`. [Online].